Spectroscopic Scanning Tunneling Microscopy Studies of Single Surface-Supported Free-Base Corroles

Mohammad Rashidi,[†] Stefan Müllegger,[*,†] Manuel Roithner,[†] Wolfgang Schöfberger,[‡] and Reinhold Koch[†]

[†]Institute of Semiconductor and Solid State Physics and [‡]Institute of Inorganic Chemistry, Johannes Kepler University Linz, 4040 Linz, Austria

S *Supporting Information*

ABSTRACT: Corroles are versatile chemically active agents in solution. Expanding their applications toward surface-supported systems requires a fundamental knowledge of corrole–surface interactions. We employed the tip of a low-temperature scanning tunneling microscope as local probe to investigate at the single-molecule level the electronic and geometric properties of surface-supported free-base corrole molecules. To provide a suitable reference for other corrole-based systems on surfaces, we chose the archetypal 5,10,15-tris(pentafluorophenyl)-corrole [H_3(TpFPC)] as model system, weakly adsorbed on two surfaces with different interaction strengths. We demonstrate the nondissociative adsorption of H_3(TpFPC) on pristine Au(111) and on an intermediate organic layer that provides sufficient electronic decoupling to investigate geometric and frontier orbital electronic properties of almost undisturbed H_3(TpFPC) molecules at the submolecular level. We identify a deviating adsorption behavior of H_3(TpFPC) compared to structurally similar porphyrins, characterized by a chiral pair of molecule–substrate configurations.

Since the first published one-pot synthesis of corroles by Gross and Paolesse in 1999,[1] corrole research has strongly increased as well as the scope of corrole applications in catalysis, photochemical sensing, molecular electronics, and biomedicine.[2] Unlike porphyrins, corroles contain a direct pyrrole–pyrrole link and three pyrrole-type hydrogens (Figure 1a) beneficial for stabilizing high-valent transition metal ions and prefer +III, +IV, and +V coordinate complexes well-suited for a number of catalytic reactions (hydroxylation of alkanes, epoxidation, sulfoxidation).[3] Corroles tend to break to open-chain structures in aerobic solution under ambient light.[4] Free-base corroles are unstable against light and air due to the reduced aromaticity and nonplanarity of the macrocycle. The stability depends on the substitution pattern of the tetrapyrrolic macrocycle and is improved by electronegative substituents. Nevertheless, certain corroles with electronegative substituents are known to degrade even at room temperature under air and ambient light.[5] The archetypal 5,10,15-tris(pentafluorophenyl)-corrole [H_3(TpFPC)], reportedly one of the most stable free-base corroles,[4a] has been intensively studied in the liquid phase (Figure 1a). H_3(TpFPC) derivatives are promising tumor inhibitors[2] and photosensitizers for solar cells.[3a]
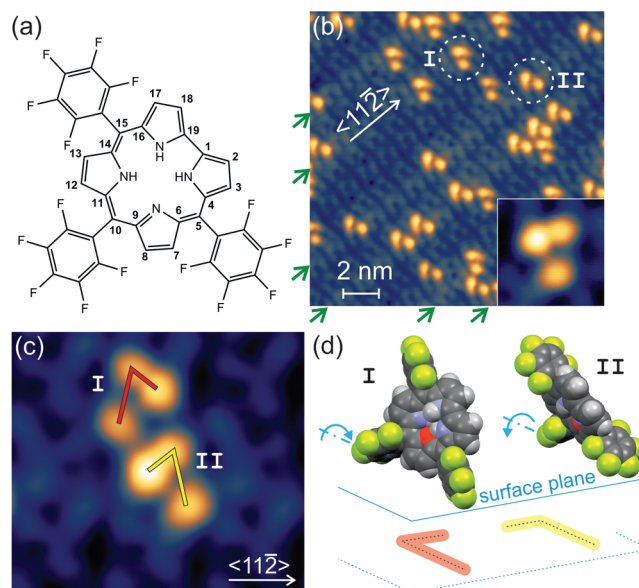
Figure 1. (a) Chemical structure of H_3(TpFPC). (b) Topographic STM overview of 1.1 monolayers H_3(TpFPC) on Au(111) (+1 V, 50 pA). The first H_3(TpFPC) monolayer is completely filled and regularly ordered (blue). Individual H_3(TpFPC) molecules of the second layer are colored orange. Circles mark single H_3(TpFPC) molecules of configurations I and II (see text). Inset: 2×2 nm² STM topograph of a single type-I admolecule. (c) Topographic STM image of type-I and type-II molecules of the second layer (4.4×3.8 nm², 1.25 V, 50 pA). (d) Adsorption model of type-I and type-II H_3(TpFPC) configurations. The nonprotonated pyrrole N is colored red for better visibility.

Here, we employ the tip of a low-temperature scanning tunneling microscope (LT-STM) as local probe to investigate at the single-molecule level the electronic and geometric properties of surface-supported H_3(TpFPC) molecules for two different weak-bonding situations: adsorbed on Au(111) or electronically decoupled by an intermediate organic layer. On both surfaces we demonstrate the nondissociative adsorption of H_3(TpFPC) and identify two different molecule–substrate configurations that are distinguishable by both the handedness of the STM topographic appearance and the energies of the unoccupied frontier molecular orbitals (MOs) observed by

scanning tunneling spectroscopy (STS). In ordered $H_3(TpFPC)$ monolayer films both chiral configurations coexist, forming an alternating sequence of homochiral rows of molecules. The observed tilted adsorption of $H_3(TpFPC)$ is distinctly different from that of porphyrins on weakly interacting surfaces.[6]

The Au(111) surface was prepared by repeated cycles of 0.5 keV Ar$^+$ bombardment and annealing at 820 K. $H_3(TpFPC)$ $(C_{37}H_{11}F_{15}N_4)$ was thermally evaporated from a thoroughly degassed quartz crucible at a source temperature of 403 K and a base pressure of <1 × 10^{-9} mbar onto Au(111) held at 300 K. STM experiments were performed at 7 K and a base pressure below 5 × 10^{-11} mbar. W tips were electrochemically etched, vacuum-annealed above 1100 K, and subsequently Au-coated by controlled indentation into the pristine gold surface.

Figure 1b shows an STM topographic image of the sample surface after deposition of ~1.1 monolayers of $H_3(TpFPC)$ on Au(111) at room temperature. A continuous layer of regularly packed $H_3(TpFPC)$ molecules is clearly discernible (blue) and evidences layer growth for the first monolayer. The characteristic double lines of the Au(111) herringbone reconstruction along the $\langle 11\overline{2}\rangle$ direction are still visible and "shine through" the $H_3(TpFPC)$ monolayer (green arrows in Figure 1b). The Au(111) reconstruction is not lifted upon adsorption, indicating, as expected, a weak molecule−substrate interaction. The regular $H_3(TpFPC)$ monolayer is aligned parallel to these lines, and domains of up to 90 nm diameter are azimuthally rotated by 120° and separated by domain boundaries along the $\langle 11\overline{2}\rangle$ direction (see Supporting Information). On top of the completed first $H_3(TpFPC)$ layer, individual $H_3(TpFPC)$ molecules and small two-dimensional clusters of $H_3(TpFPC)$ molecules are observed (orange). Circles in Figure 1b show single $H_3(TpFPC)$ molecules in the second layer. We employ this particular sample configuration to study single $H_3(TpFPC)$ molecules weakly bound with different interaction strengths: those in direct contact with the metal that modifies and rearranges the frontier orbital electronic structure,[7] and those decoupled[8] by the underlying organic (first) monolayer, allowing us to obtain topographic and electronic information about almost undisturbed single $H_3(TpFPC)$ molecules, similar to the gas phase.

First, we focus on single $H_3(TpFPC)$ molecules of the second layer. At positive bias voltages from about +1 to +1.5 V, STM topographs reveal a characteristic three-lobe shape of single $H_3(TpFPC)$ molecules, each lobe having a different apparent height (Figure 1b inset). By comparing the measured lobe−lobe separations with those of the molecular structure, we attribute the three lobes to the fluorophenyl *meso*-substituents (further corroborated by our STS data, below). A flat-on adsorption configuration of $H_3(TpFPC)$ with the tetrapyrrolic macrocycle parallel to the substrate plane would imply an STM contour with C_2 symmetry (Figure 1a). The observed C_1 symmetry of the STM contours of Figure 1b indicates that the $H_3(TpFPC)$ molecules are tilted with respect to the substrate. Each molecule lies edge-on with two fluorophenyls closer to the interface and the third one above, which appears as the most intense lobe in STM topographs (Figure 1b inset). From the side-to-side ratio of the STM contour a tilt angle of ~50° is estimated.

Intriguingly, two chiral molecule−substrate configurations are observed by STM, manifested by two L-shaped contours that are both mirrored and rotated with respect to each other. This is best seen in Figure 1c, displaying a surface area with two

adjacent second-layer molecules marked by red and yellow L lines as guides to the eye. The model in Figure 1d explains the existence of these two configurations: a side-tilt about the lower edge of the molecule to either the right or left side, labeled I and II, respectively. Two additional chiral configurations (not shown) are obtained when the 10,15 fluorophenyls are closest to the substrate instead of the 5,10 displayed in Figure 1c. We remark, however, that from our experimental results we cannot distinguish whether the two chiral configurations observed by STM are two different enantiomers (or atropisomers) or just two molecules oriented differently with respect to the substrate plane, or mixtures of both.

The STS results in Figure 2 unveil the frontier orbital electronic properties of electronically decoupled $H_3(TpFPC)$
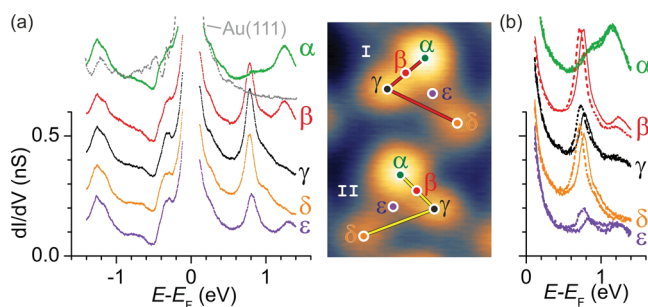
Figure 2. Constant-current tunneling spectra of decoupled single $H_3(TpFPC)$ molecules in the second layer (100 pA). (a) For configuration I, spectra over different intramolecular positions, $\alpha-\varepsilon$, of the STM image taken from Figure 1a (right side). The dashed line is the spectrum of pristine Au(111). (b) Empty-state regime of configurations I (solid) and II (dashed).

molecules in the second layer. The local differential tunneling conductance, dI/dV, was recorded in constant-current mode (active feedback loop). The dI/dV signal was obtained with lock-in technique and a sinusoidal modulation peak-to-peak voltage of V_{pp} = 20 mV and 700 Hz added to V, averaging 10 consecutively recorded spectra. Reliable judgment of the cleanliness and condition of our STM tips was based on routinely monitoring the dI/dV signature of the Au(111) surface state obtained over pure substrate regions and comparing its position and shape with literature values.

Figure 2a displays tunneling spectra recorded at well-selected tip positions labeled $\alpha-\varepsilon$ over different submolecular units of second-layer type-I $H_3(TpFPC)$. Enhanced conductance is observed at certain energies independent of the tip position. We start with the spectrum at position γ. Comparison with the spectrum of pristine Au(111) (dashed line in Figure 2a) enables us to distinguish substrate-related features from resonant tunneling through distinct frontier MOs of $H_3(TpFPC)$. In the energy range from about −0.8 to +0.6 eV, the spectrum resembles that of pristine Au(111). The shoulder around −0.5 eV corresponds to the onset of the Au(111) surface-state band and indicates direct tunneling between tip and metal substrate. Note that constant-current spectroscopy leads to point contact when the bias voltage approaches zero, causing the sharp increase of the signal observed in the respective energy range. The distinctly discernible resonances at higher/lower energies are attributed to resonant tunneling through distinct MOs of $H_3(TpFPC)$. The respective peak energies are listed in Table 1. The peaks at −1.15 and +0.79 eV are attributed to HOMO and LUMO,

**Table 1. STS Peak Energies (in eV) of H$_3$(TpFPC) Molecules in the First and Second Layers[a]**

	second layer		first layer	
	I	II	I	II
HOMO−1	−1.25	−1.25	(−1.1)	(−1.1)
HOMO	−1.15	−1.15	−0.85	−0.85
LUMO	+0.79	+0.72	+1.29	+1.20
LUMO+1	+1.00	(+0.9)	+1.41	+1.44
LUMO+2	+1.25	+1.15	+1.80	+1.72

[a]The estimated experimental error is ±0.05 eV.

yielding a respective energy gap of 1.9(4) eV, in very good agreement with the HOMO/LUMO gap of 1.91 eV measured by UV/vis spectroscopy in solution.[9]

At other tip positions the HOMO/LUMO intensity is lowered, indicating weaker overlap of specific MOs with the STM tip in constant-current mode. Spectrum α clearly differs from the others by the very weak LUMO and LUMO+1 signals, indicating that the STM tip over the "high" fluorophenyl (farthest away from the surface) no longer overlaps with the LUMO and LUMO+1, in accordance with the localization of LUMO (and HOMO) over the macrocycle known from free-base corroles[10] and metallocorroles.[11] To rationalize our experimental results we performed DFT single-point energy calculations of a single H$_3$(TpFPC) molecule with the Gaussian 03 package[12] using Becke's three-parameter hybrid functional (B3LYP),[13] Pople's 6-311+G(d,p) compound basis set,[14] and a fixed conformation of the H$_3$(TpFPC) obtained from bulk-phase data.[1c]

Although the predictive quality of DFT-calculated MO energies is generally poor,[7] the symmetry and spatial extent of MOs typically are reliable and hence useful for interpreting our experimental data. Figure 3 displays our DFT results for
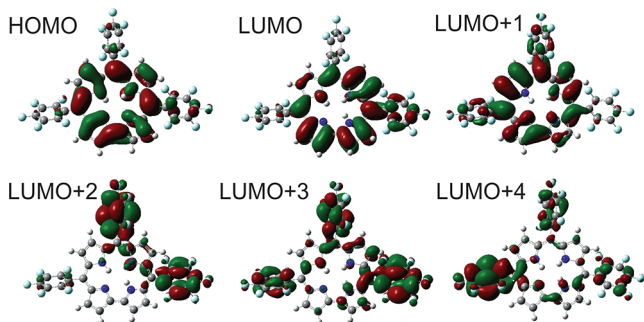

Figure 3. DFT-calculated MOs of an isolated H$_3$(TpFPC) molecule.

selected MOs. LUMO and LUMO+1 are mainly localized over the corrole macrocycle, while the almost degenerate LUMO+2, +3, and +4 are restricted to the fluorophenyl substituents. This corroborates the above interpretation of spectrum α, where electrons tunnel mainly into the almost degenerate LUMO+2, +3, and +4, in agreement with the tilted adsorption configuration derived from our STM images.

Figure 2b compares spectra of type-I (solid) and type-II (dashed) molecules recorded over equal positions α−ε. Intriguingly, the unoccupied frontier MOs of type-II molecules are significantly shifted by ~70−100 meV toward lower energies (see Table 1), whereas the occupied MOs are almost unaffected (not shown). These energy shifts are characteristic of type-II configuration and allow us to unambiguously

distinguish type-I and type-II configurations by STS. The observed shifts may be due to the nonequivalent adsorption positions of fluorophenyls and pyrroles relative to the underlying surface, with opposite sides of the nonplanar macrocycle (due to the H arrangement) facing the surface (Figure 1d), which may modify the molecular buckling. In a recent study we found that in buckled porphyrins on Au(111) slight geometric variations of the macrocycle can give rise to energy shifts of up to 200 meV.[15]

In the following we discuss the structural properties of the regular first H$_3$(TpFPC) monolayer on Au(111), shown in Figure 4a at different bias voltages. Note the almost identical
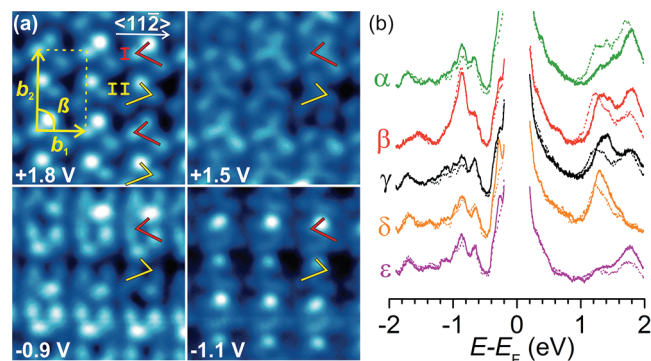
Figure 4. (a) STM topographs (5.2×5.2 nm^2, 50 pA) of the first H$_3$(TpFPC) monolayer on Au(111) recorded at different bias voltages; the surface unit cell is overlaid (yellow). (b) Constant-current tunneling spectra recorded at selected tip positions (defined in Figure 2a), α−ε, over type-I (solid lines) and type-II (dotted lines) configurations of H$_3$(TpFPC) in the first monolayer.

STM topography of single H$_3$(TpFPC) molecules observed in the first monolayer at the LUMO−2 energy of +1.8 V (Figure 4a, top left) and at +1.25 V in the second layer (Figure 1c), indicating similar side-tilted orientations of the respective H$_3$(TpFPC) molecules. Compared to the second layer, the bias dependence of the STM topographs in Figure 4a reflects the different bonding situation (interaction strength) at the molecule−Au(111) interface of the first layer, where the energies of specific MOs (probed by the tunneling electrons) are shifted (Table 1). No significant effect on the STM topographs or the STS data was observed due to the Au(111) herringbone reconstruction (periodic modulation of the substrate lattice between fcc- and hcp-type packing). Near the energy of LUMO+2, the three fluorophenyl substituents of each H$_3$(TpFPC) molecule can be discerned (images at +1.8 and +1.5 V). The same molecular units also dominate the topographic contrast near the HOMO energy, where the relative intensities have changed (image at −0.9 V). Finally, the corrole macrocycle becomes visible at energies slightly below the HOMO, causing a distinct change of the topography (image at −1.1 V).

As in the second layer, we observed that H$_3$(TpFPC) molecules in the first monolayer exhibit either type-I or type-II configuration (Figure 4a, red and yellow L lines). Figure 4b juxtaposes the tunneling spectra of type-I (solid) and type-II (dashed) molecules recorded over intramolecular positions α−ε, taken analogously to Figure 2a. The respective spectra are qualitatively similar to those of the decoupled second layer (compare with Figure 2), but the MO resonances are shifted toward higher energies by ~0.3−0.4 eV and the HOMO/

LUMO gap is increased by 0.11 eV (see Table 1). Most likely, this is caused by the different work functions of the respective surfaces, affecting the surface dipole layer at the interface. The weak LUMO+2 resonance at positions δ and γ (also observed in the second layer, see Figure 2) indicates that the respective fluorophenyls are closer to the substrate, in accordance with a tilted adsorption of H_3(TpFPC) (Figure 1d).

The first monolayer exhibits a stripe pattern aligned along the $\langle 11\bar{2}\rangle$ direction of Au(111) (Figure 1b) that originates from a lateral sequence of ordered rows of H_3(TpFPC) molecules with alternating type-I or type-II configuration. This regular pattern can be recognized in the STM images of Figure 4a, from which we have determined the parameters of the corresponding surface unit cell: $|b_1|$ = 1.5(1) nm, $|b_2|$ = 2.4(0) nm, and β = 90° ± 2°. The epitaxy matrix of the H_3(TpFPC) monolayer relative to the rectangular unit cell of the $22\times(3)^{1/2}$ reconstructed Au(111) lattice reads $C \approx \left(\begin{smallmatrix} 0.24 & 0 \\ 0 & 0.53 \end{smallmatrix}\right)$. The rational numbers indicate a coincident[16] registry of the H_3(TpFPC) monolayer with respect to the reconstructed Au(111) lattice. Although in the first monolayer it seems possible to accommodate two flat-lying molecules per unit cell without mutual steric hindrance, the observed side-tilt indicates a less dense packing. This can be explained by mutual repulsion between neighboring H_3(TpFPC) molecules, similar to that observed for comparable hydrocarbon molecules on weakly interacting surfaces.[17] The H_3(TpFPC) molecules seem to lower their mutual repulsion by tilting away from the surface plane, similar to the molecules of the second layer (discussed above) and similar to the bulk structure exhibiting parallel rows of regularly π-stacked H_3(TpFPC) molecules in the [010] direction.[1c] We remark that the observed layer-like growth mode of side-tilted H_3(TpFPC) molecules on Au(111) is distinctly different from the flat-on adsorption on weakly interacting surfaces reported for metallocorrole complexes[18] and for many free-base[6a–d] and metalloporphyrins.[6e,f,15,19]

In conclusion, we have characterized for the first time H_3(TpFPC) adsorbed on two different weakly interacting surfaces on the submolecular scale by LT-STM and STS, providing structural and electronic properties of almost undisturbed single H_3(TpFPC) molecules. Our study reveals a deviating adsorption behavior of free-base corroles, compared to structurally similar porphyrins, with two different chiral molecule–substrate configurations clearly distinguished by STS. Our data may serve as reference for other corrole-based systems on surfaces and will have an impact on the future development of surface-supported corrole applications.

■ ASSOCIATED CONTENT

Ⓢ Supporting Information

Experimental details and complete ref 12. This material is available free of charge via the Internet at http://pubs.acs.org.

■ AUTHOR INFORMATION

Corresponding Author

stefan.muellegger@jku.at

■ ACKNOWLEDGMENTS

■ REFERENCES

(1) (a) Gross, Z.; Galili, N.; Saltsman, I. *Angew. Chem.* **1999**, *111*, 1530. (b) Gross, Z.; Galili, N. *Angew. Chem., Int. Ed.* **1999**, *38*, 2366. (c) Gross, Z.; Galili, N.; Simkhovich, L.; Saltsman, I.; Botoshansky, M.; Blaser, D.; Boese, R.; Goldberg, I. *Org. Lett.* **1999**, *1*, 599. (d) Paolesse, R.; Jaquinod, L.; Nurco, D. J.; Mini, S.; Sagone, F.; Boschia, T.; Smith, K. M. *Chem. Commun.* **1999**, 1307.

(2) Aviv-Harel, I.; Gross, Z. *Chem. Eur. J.* **2009**, *15*, 8382.

(3) (a) Aviv, I.; Gross, Z. *Chem. Commun.* **2007**, 1987. (b) Grodkowski, J.; Neta, P.; Fujita, E.; Mahammed, A.; Simkhovich, L.; Gross, Z. *J. Phys. Chem. A* **2002**, *106*, 4772.

(4) (a) Geier, G. R.; Chick, J. F. B.; Callinan, J. B.; Reid, C. G.; Auguscinski, W. P. *J. Org. Chem.* **2004**, *69*, 4159. (b) Ding, D.; Harvey, J. D.; Ziegler, C. J. *J. Porphyrins Phthalocyanines* **2005**, *9*, 22. (c) Tardieux, C.; Gros, C. P.; Guilard, R. *J. Heterocycl. Chem.* **1998**, *35*, 965.

(5) Barata, J. F. B.; Neves, M. G. P. M. S.; Tome, A. C.; Faustino, M. A. F.; Silva, A. M. S.; Cavaleiro, J. A. S. *Tetrahedron Lett.* **2010**, *51*, 1537.

(6) (a) Buchner, F.; Schwald, V.; Comanici, K.; Steinrück, H. P.; Marbach, H. *ChemPhysChem* **2007**, *8*, 241. (b) Shubina, T. E.; Marbach, H.; Flechtner, K.; Kretschmann, A.; Jux, N.; Buchner, F.; Steinrück, H. P.; Clark, T.; Gottfried, J. M. *J. Am. Chem. Soc.* **2007**, *129*, 9476. (c) Scarselli, M.; Castrucci, P.; Monti, D.; De Crescenzi, M. *Surf. Sci.* **2007**, *601*, 5526. (d) Auwärter, W.; Klappenberger, F.; Weber-Bargioni, A.; Schiffrin, A.; Strunskus, T.; Wöll, C.; Pennec, Y.; Riemann, A.; Barth, J. V. *J. Am. Chem. Soc.* **2007**, *129*, 11279. (e) Auwarter, W.; Weber-Bargioni, A.; Riemann, A.; Schiffrin, A.; Groning, O.; Fasel, R.; Barth, J. V. *J. Chem. Phys.* **2006**, *124*, 194708. (f) Buchner, F.; Warnick, K.-G.; Wölfle, T.; Görling, A.; Steinrück, H.-P.; Hieringer, W.; Marbach, H. *J. Phys. Chem. C* **2009**, *113*, 16450. (g) Müllegger, S.; Schöfberger, W.; Rashidi, M.; Lengauer, T.; Klappenberger, F.; Diller, K.; Kara, K.; Barth, J. V.; Rauls, E.; Schmidt, W. G.; Koch, R. *ACS Nano* **2011**, *5*, 6480.

(7) (a) Neaton, J.; Hybertsen, M.; Louie, S. *Phys. Rev. Lett.* **2006**, *97*, 216405. (b) Thygesen, K. S.; Angel Rubio, A. *Phys. Rev. Lett.* **2009**, *102*, 046802.

(8) Repp, J.; Meyer, G.; Stojkovic, S. M.; Gourdon, A.; Joachim, C. *Phys. Rev. Lett.* **2005**, *94*, 026803.

(9) Bendix, J.; Dmochowski, I.; Gray, H.; Mahammed, A.; Simkhovich, L.; Gross, Z. *Angew. Chem., Int. Ed.* **2000**, *39*, 4048.

(10) Hocking, R. K.; DeBeer George, S.; Gross, Z.; Walker, F. A.; Hodgson, K. O.; Hedman, B.; Solomon, E. I. *Inorg. Chem.* **2009**, *48*, 1678.

(11) (a) Alemayehu, A. B.; Gonzalez, E.; Hansen, L. K.; Ghosh, A. *Inorg. Chem.* **2009**, *48*, 7794. (b) Aviv-Harel, I.; Gross, Z. *Coord. Chem. Rev.* **2011**, *255*, 717. (c) Reith, L. M.; Stiftinger, M.; Monkowius, U.; Knör, G.; Schoefberger, W. *Inorg. Chem.* **2011**, *50*, 6788.

(12) Frisch, M. J. et al. *Gaussian 03*, Revision E.01; Gaussian, Inc.: Wallingford, CT, 2004.

(13) Becke, A. D. *J. Chem. Phys.* **1993**, *98*, 5648.

(14) (a) Frisch, M. J.; Pople, J. A.; Binkley, J. S. *J. Chem. Phys.* **1984**, *80*, 3265. (b) Krishnan, R.; Binkley, J. S.; Seeger, R.; Pople, J. A. *J. Chem. Phys.* **1980**, *72*, 650.

(15) Müllegger, S.; Rashidi, M.; Lengauer, T.; Rauls, E.; Schmidt, W. G.; Knör, G.; Schöfberger, W.; Koch, R. *Phys. Rev. B* **2011**, *83*, 165416.

(16) Hooks, D.; Fritz, T.; Ward, M. *Adv. Mater.* **2001**, *13*, 227.

(17) (a) Müllegger, S.; Salzmann, I.; Resel, R.; Winkler, A. *Appl. Phys. Lett.* **2003**, *83*, 4536. (b) Müllegger, S.; Winkler, A. *Surf. Sci.* **2005**, *574*, 322.

(18) Kuck, S.; Hoffmann, G.; Broering, M.; Fechtel, M.; Funk, M.; Wiesendanger, R. *J. Am. Chem. Soc.* **2008**, *130*.

(19) Müllegger, S.; Schöfberger, W.; Rashidi, M.; Reith, L. M.; Koch, R. *J. Am. Chem. Soc.* **2009**, *131*, 17740.